Mineralium Deposita (2005) 39: 845–863
DOI 10.1007/s00126-004-0457-5

ARTICLE

Werner E. Halter · Christoph A. Heinrich
Thomas Pettke

Magma evolution and the formation of porphyry Cu–Au ore fluids: evidence from silicate and sulfide melt inclusions

Received: 9 June 2004 / Accepted: 17 November 2004 / Published online: 20 January 2005

Abstract Silicate and sulfide melt inclusions from the andesitic Farallón Negro Volcanic Complex in NW Argentina were analyzed by laser ablation ICPMS to track the behavior of Cu and Au during magma evolution, and to identify the processes in the source of fluids responsible for porphyry-Cu-Au mineralization at the 600 Mt Bajo de la Alumbrera deposit. The combination of silicate and sulfide melt inclusion data with previously published geological and geochemical information indicates that the source of ore metals and water was a mantle-derived mafic magma that contained approximately 6 wt.% H_2O and 200 ppm Cu. This magma and a rhyodacitic magma mixed in an upper-crustal magma chamber, feeding the volcanic systems and associated subvolcanic intrusions over 2.6 million years. Generation of the ore fluid from this magma occurred towards the end of this protracted evolution and probably involved six important steps: (1) Generation of a sulfide melt upon magma mixing in some parts of the magma chamber. (2) Partitioning of Cu and Au into the sulfide melt (enrichment factor of 10,000 for Cu) leading to Cu and Au concentrations of several wt.% or ppm, respectively. (3) A change in the tectonic regime from local extension to compression at the end of protracted volcanism. (4) Intrusion of a dacitic magma stock from the upper part of the layered magma chamber. (5) Volatile exsolution and resorption of the sulfide melt from the lower and more mafic parts of the magma chamber, generating a fluid with a Cu/Au ratio equal to that of the precursor sulfide. (6) Focused fluid transport and precipitation of the two metals in the porphyry, yielding an ore body containing Au and Cu in the proportions dictated by the magmatic fluid source. The Cu/S ratio in the sulfide melt inclusions requires that approximately 4,000 ppm sulfur is extracted from the andesitic magma upon mixing. This exceeds the solubility of sulfide or sulfate in either of the silicate melts and implies an additional source for S. The extra sulfur could be added in the form of anhydrite phenocrysts present in the rhyodacitic magma. It appears, thus, that unusually sulfur-rich, not Cu-rich magmas are the key to the formation of porphyry-type ore deposits. Our observations imply that dacitic intrusions hosting the porphyry–Cu–Au mineralization are not representative of the magma from which the ore-fluid exsolved. The source of the ore fluid is the underlying more mafic magma, and unaltered andesitic dikes emplaced immediately after ore formation are more likely to represent the magma from which the fluids were generated. At Alumbrera, these andesitic dikes carry relicts of the sulfide melt as inclusions in amphibole. Sulfide inclusions in similar dykes of other, less explored magmatic complexes may be used to predict the Au/Cu ratio of potential ore-forming fluids and the expected metal ratio in any undiscovered porphyry deposit.

Keywords Porphyry · Copper · Gold · Sulfide · Melt inclusions · Fluid · Andesite · Alumbrera · Argentina

Editorial handling: B. Lehmann

W. E. Halter (✉) · C. A. Heinrich · T. Pettke
Isotope Geochemistry and Mineral Resources, Department of Earth Sciences, ETH Zürich, 8092 Zurich, Switzerland
E-mail: halter@erdw.ethz.ch
Tel.: +41-1-6326802
Fax: +41-1-6321827

Introduction

Due to their economic significance, porphyry-type ore deposits have been intensely investigated worldwide and much is known about the ore-forming environment and the causes for metal precipitation (Lowell and Guilbert 1970; Sillitoe 1973; Gustafson and Hunt 1975; Dilles 1987; Hezarkhani et al. 1999; Ulrich et al. 2001; Ulrich and Heinrich 2001; Kesler et al. 2002). From recent studies (Stefanini and Williams-Jones 1996; Audetat et al. 1998; Hezarkhani et al. 1999; Heinrich et al. 2004), it appears that processes at the depositional site control

the distribution of the metals and the ore grades, but the composition (i.e., the Au/Cu ratio) of the ore seems to be governed by the composition of the primary magmatic fluid as it exsolves from the melt (Ulrich et al. 1999). Thus, to explain the variability in the composition of magmatic-hydrothermal ores, we need to understand the processes at the source of the ore fluids, which are closely related to the history of entire ore-forming magmatic systems up to the point of volatile saturation.

To address this question, we reconstructed the evolution of the Farallón Negro Volcanic Complex (FNVC) in northwestern Argentina (Llambías 1970; Sasso 1997; Halter et al. 2004a; Harris et al. 2004) which generated the large Bajo de la Alumbrera porphyry-Cu–Au deposit (Sillitoe 1973; Bassi and Rochefort 1980; Stults 1985; Guilbert 1995; Proffett 2003; Ulrich and Heinrich 2001; Harris et al. 2003). Our results are published in a series of four papers that report the discovery of sulfide melt inclusions (Halter et al. 2002a) and successively established the microanalytical technique (Halter et al. 2004c), the evolution of the magmatic complex based on field mapping, whole-rock chemical and isotopic analysis and $^{40}Ar/^{39}Ar$ geochronology by stepwise laser heating (Halter et al. 2004a), and the origin of andesitic magmas through mixing of basalt and rhyodacite (Halter et al. 2004b).

The combination of geological constraints on the magmatic evolution of the complex with the mass balance and fluid-chemical requirements imposed by the formation of the 600 Mt ore deposit permits a detailed reconstruction of the timing of volatile saturation, the consequences of sulfide melt saturation, the source for the hydrothermal fluid and the chronology of the ore-forming events. Here, we use this geological and geochemical framework to determine the source magmas for fluids, ore metals, and sulfur, and to trace the behavior of Cu and Au during magma evolution. Our results contrast with current views of the processes responsible for ore-fluid formation, which generally assume that porphyry-mineralizing magmas have to be sulfide-undersaturated to permit metal enrichment, and they have the potential of practical application to regional mineral exploration.

Geological setting

The FNVC is located in the Catamarca Province of northwestern Argentina, ~200 km east of the present Andean volcanic arc and 500 km from the trench. It lies in the Sierras Pampeanas province, close to the southwestern margin of the Puna plateau and is the easternmost manifestation of Late Tertiary volcanic activity related to the subduction of the Nazca plate beneath South America. The contact between the Sierras Pampeanas and the Puna plateau is marked by the NE–SW striking crustal-scale Tucuman Transfer Zone (Urreiztieta et al. 1993). This structure probably controlled magma ascent along local dilatancies (Sasso 1997). Late Miocene tectonic activity in the Sierras Pampeanas was dominated by broad regions of basement uplifts forming kilometer-scale blocks (Jordan and Allmendinger 1986; Allmendinger 1986). Uplift occurred as a result of regional compression since the late Miocene (Coughlin et al. 1998). Associated reverse faults subdivided the FNVC into several zones with various degrees of uplift, exposing volcanic and subvolcanic intrusive rocks at variable levels (Llambías 1970; Halter et al. 2004a).

Previous mapping and analysis of this system (Llambías 1970; Sasso 1997; Proffett 2003; Halter et al. 2004a) show that the complex represents the remnants of a 20 km wide and 4,500 m high stratovolcano (Sillitoe 1973; Halter et al. 2004a), intruded by numerous subvolcanic stocks (Fig. 1). Volcanic units dip away from a large central stock (Alto de la Blenda), interpreted to be the main volcanic conduit. Extensive erosion removed over 3,500 m of the vertical topography of the edifice (Ulrich 1999) and exposed the deep, internal parts of the volcano. The base of this stratovolcano against underlying Palaeozoic metasediments has recently been reached by drilling some 500 m below pre-mine land surface at Alumbrera (S. Brown and Minera Alumbrera, personal communications). The present study focused on the largest and the best-exposed part of the complex (Fig. 1), which records most of the intrusive and hydrothermal events, including a profile through the volcanic rocks from the central stock towards the northwest, and the Bajo de la Alumbrera deposit located ~3 km southeast of the inferred center of the volcano. Most of the volcanic pile could be sampled in sequence from the interior to the rim of the volcanic complex. $^{40}Ar/^{39}Ar$ stepwise laser heating geochronology is consistent with this interpretation and allowed determination of absolute timing of subvolcanic intrusions within this sequence (Halter et al. 2004a).

Evolution of the magmatic complex based on previous studies

Based on extensive field observations (Figs. 1, 2), whole-rock geochemistry, $^{40}Ar/^{39}Ar$ stepwise laser heating ages of amphiboles and biotites and microanalysis of melt inclusions, we have reconstructed the evolution of the FNVC from the beginning of volcanism at 9.7 Ma to the last subvolcanic intrusion emplaced at 6.1 Ma (Halter et al. 2004a, b) as summarized in the following sections. We will distinguish "stocks" representing a set of intrusions emplaced in a restricted area and probably within a short period of time, from individual "intrusions" as distinct magma emplacement events.

Emplacement of intrusive and extrusive rocks

The volcanic rocks are mainly high-potassium calcalkaline basalts, basaltic andesites and andesites, containing 45–66 wt.% SiO_2 and phenocryst assemblages

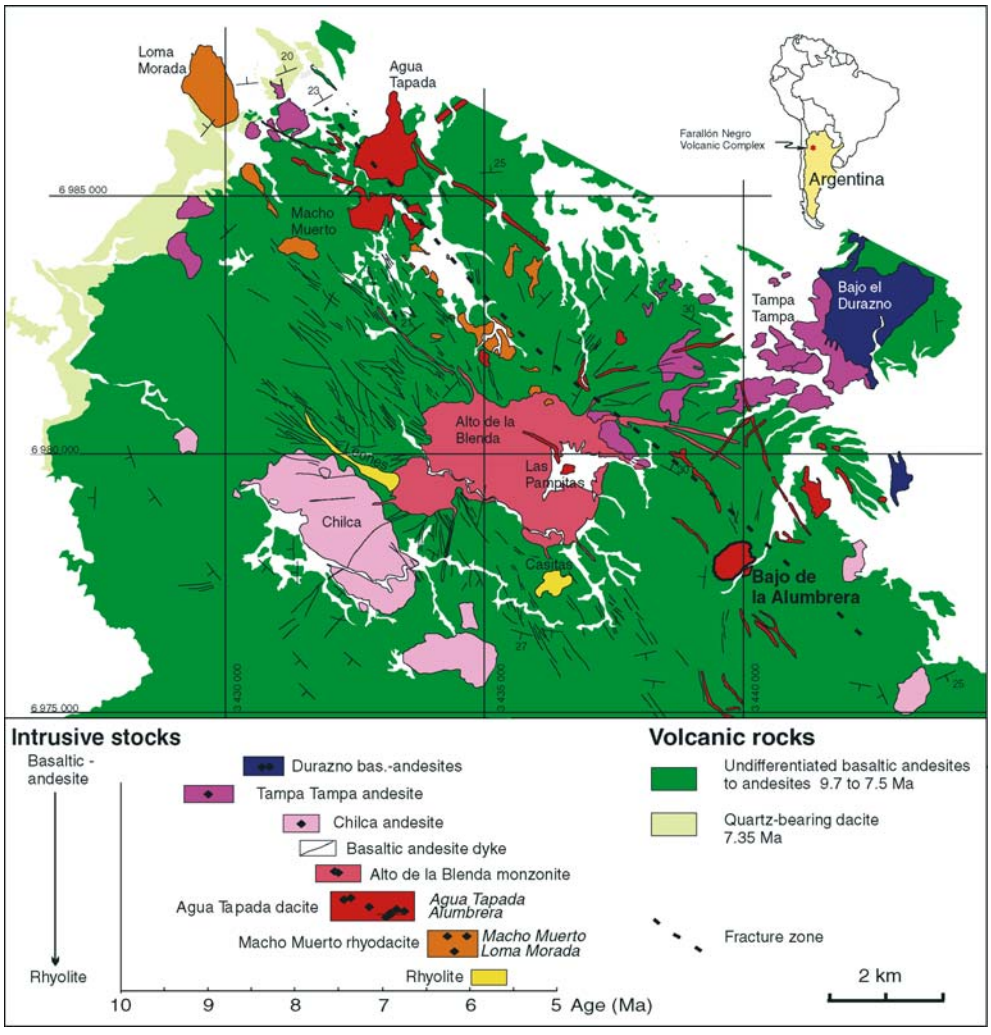

Fig. 1 Map of northwestern part of the Farallón Negro Volcanic Complex showing the horizontally eroded stratovolcano and subvolcanic stocks. The volcanic rocks are mainly basaltic andesites and andesites, with some dacites northwest of Agua Tapada. Intrusions range from basaltic andesites to rhyolites. Also shown are $^{40}Ar/^{39}Ar$ stepwise laser heating ages determined for intrusive rocks (*black diamonds*), reported by Halter et al. (2004a)

of amphibole + plagioclase + magnetite ± pyroxene. Andesites are by far the most abundant extrusive rocks. Geological reconstruction of the volcanic stratigraphy and numerous $^{40}Ar/^{39}Ar$ age data (Sasso 1997; Halter et al. 2004a) indicate an approximately steady extrusion rate of basaltic andesite and andesite of the order of 300 km^3 per million years. over an extended period of ~2.2 million years between 9.7 Ma and 7.5 Ma. Biotite-bearing volcanic rocks appeared only after 8.0 Ma. The main volcanic activity ceased at 7.5 Ma with the crystallization of the equigranular Alto de la Blenda stock, interpreted to be the central volcanic conduit (Llambías 1972). The only younger extrusive rocks are quartz-bearing dacitic ignimbrites extruded in a flank eruption at 7.35 Ma (Fig. 1). The coeval Agua Tapada stock is the likely intrusive feeder, as indicated by dykes connecting it to the ignimbrite. This event is associated with a partial caldera collapse on the northwestern side of the complex (Llambías 1972; Sasso 1997; Bain 2001; Halter et al. 2004a).

Subvolcanic stocks were first emplaced at 9.0 Ma and became abundant after 8.5 Ma. Individual stocks consist of one to eight intrusions (Fig. 2), emplaced within a restricted time frame, but comprising a wide range in compositions. Stocks are mostly dacitic but range from andesitic to rhyolitic and contain amphibole + plagioclase + magnetite ± pyroxene or plagioclase + quartz + magnetite ± amphibole ± biotite as the main phenocryst phases. Pyroxene is restricted to stocks prior to 7.5 Ma and represents at most 10 vol.% of phenocrysts. Biotite appears as a major phenocryst phase in stocks after 7.5 Ma. Amphibole is ubiquitous in all fresh intrusive stocks, except in the latest and the most silica-rich ones dominated by biotite, and commonly shows resorption or oxidation rims.

In the first million years of magmatic activity, the composition of extrusive rocks varied randomly between basaltic andesites and andesites. Rapid changes in bulk-rock chemistry suggest that no significant magma chamber was established at this stage (Dungan et al. 2001). Some 1.2 million years after initiation of extrusive activity, a continuous compositional evolution of subvolcanic intrusions with time is taken as evidence for the gradual build-up and growth of a subvolcanic magma chamber heated by continued advection of magma through the center of the volcano.

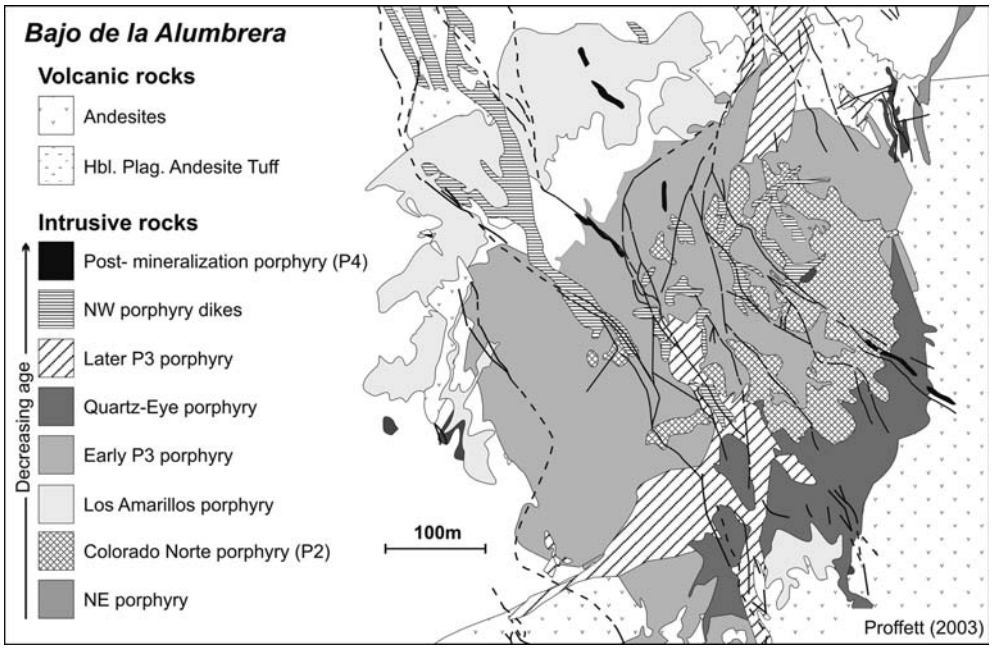

Fig. 2 Geological map of the Alumbrera porphyry deposit after Proffett (2003). The succession of intrusions shows an evolution from early dacites to late andesites between 7.1 Ma and 6.7 Ma. Sulfide melt inclusions are found in post mineralization andesite dykes

Cessation of the main volcanic activity at 7.5 Ma was probably caused by the end of magma supply to the chamber, concurrently ending the heat supply and forcing the system to progressively crystallize. Following this event, only dacitic and more silica-rich intrusive rocks were emplaced. The spatial distribution of these intrusions is not random as during the previous 2 million years but follows a NW–SE trend (Fig. 1) becoming progressively younger towards the SE, from Agua Tapada (7.35 Ma) through Las Pampitas (7.2 Ma) to Alumbrera (7.1–6.7 Ma). This suggests a change in the tectonic regime from locally extensive (Sasso and Clark 1998) to dominantly transpressive. Compression probably contributed to stopping the extrusive activity, and constrained the magma chamber to evolve internally towards bulk fluid saturation. The NE–SW alignment corresponds to a fracture zone that controlled localized ascent of volatile-saturated magma.

Melt inclusions and magma mixing

Silicate melt inclusions are trapped in amphibole, pyroxene, plagioclase and quartz and are generally crystallized (Fig. 3). Their compositional range and variability as a function of their silica content overlaps that of bulk rocks for all major and most trace elements (Fig. 4). However, melt inclusions depict a dominantly bimodal distribution with either basaltic or rhyodacitic compositions, in strong contrast to the predominately andesitic bulk rock compositions. Basaltic melt inclusions are mostly trapped in amphibole, whereas silica-rich melt inclusions are found almost exclusively in plagioclase and quartz. Thus, melt inclusions in different phenocrysts from the same rock commonly depict highly contrasting compositions (Fig. 5). The composition of the bulk rock is generally intermediate between that of the melt inclusions (Halter et al. 2004b). This shows that phenocryst minerals observed in a given rock crystallized from different melts, and are in fact xenocrysts in the bulk rock. These observations and linear compositional variations of intrusive and extrusive rocks (Fig. 4) are best explained by a process of mixing varying proportions of a mafic and a felsic (rhyodacitic) magmas that already contained phenocrysts. The mafic component is preserved as melt inclusions with 42–45 wt.% SiO_2 in amphibole only, suggesting that amphibole and magnetite (also present as inclusions in amphibole) were the only phases to crystallize from the mafic melt, at temperatures of approximately 1,000°C, high pressure (> 350 MPa) and high water contents close to saturation (6.0 wt.% H_2O; Moore and Carmichael 1998). Trace-element composition and isotopic data suggest that this magma is derived from the mantle (Becker 2001; Halter et al. 2004a, b). Plagioclase dominantly crystallized from the felsic magma prior to mixing, as rhyodacitic melt inclusions are present almost exclusively in this phase. Both magmas may have been at similar temperatures and viscosities, thanks to the high H_2O content of the mafic magma, thus favoring complete hybridization of the melts by preventing the mafic magma from rapid solidification (Sparks and Marshall 1986).

Endmembers of the mixing process appear to be the same in intrusive and extrusive rocks, which overlap in their time of emplacement, in their spatial distribution, and in their chemical and isotopic compositional range, demonstrating a common source for intrusive and extrusive rocks. However, intrusions and extrusions have characteristic differences, evidenced by a systematic distinction in the compositions of intermediate melt inclusions and in their occurrence in the various phases. These differences indicate that intrusions and volcanic

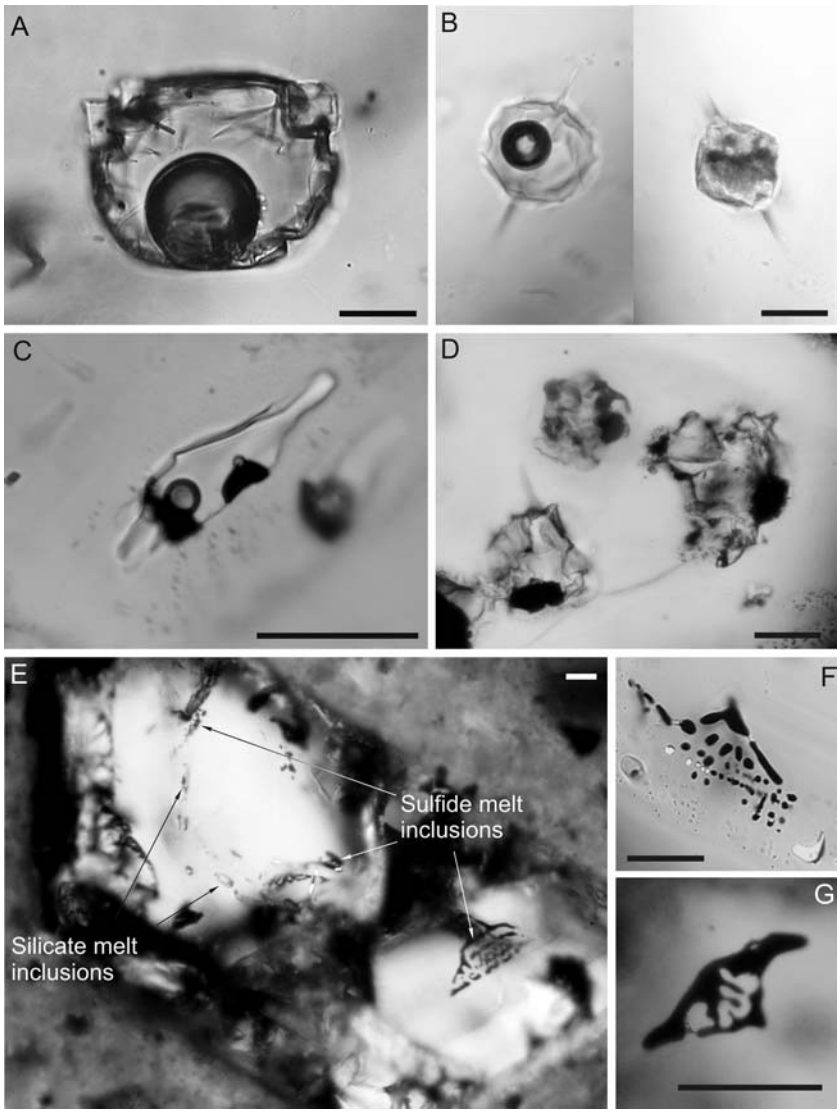

Fig. 3 Microphotographs of silicate and sulfide melt inclusions in various host phases. **A** Partially crystallized melt inclusions in plagioclase. **B**Melt inclusions in quartz with various degrees of crystallization. **C** Melt inclusion in amphibole with some daughter phases. **D** Crystallized melt inclusions in pyroxene. **E** Silicate and sulfide melt inclusions in amphibole. **F** and **G** show enlargements of sulfide melt inclusions. *Scale bars* are 10 μm

eruptions tapped different regions of a common magma chamber, presumably at slightly different times.

In volcanic rocks, intermediate melts generated upon mixing are mainly recorded in plagioclase and pyroxene. Amphiboles mainly host melt inclusions of mafic composition, suggesting that this phase was not extensively growing during the mixing process that generated most of the extrusive andesites. Inclusions in pyroxene indicate that this phase formed in melts with a restricted compositional range between 50 wt.% $SiO_2$and 55 wt.% SiO_2 , produced by magma mixing. Textural evidence and chemically similar melt inclusions show that plagioclase crystallized together with this pyroxene (Halter et al. 2004b). In rocks where pyroxene and plagioclase coexist, amphibole is partially resorbed, indicating a shift from an amphibole (±plagioclase) stable assemblage to the plagioclase + pyroxene stability field. In water-saturated melts of intermediate composition, the latter assemblage is stable at pressures below 150 MPa and temperatures around 950°C (Moore and Carmichael 1998). Thus, the replacement of amphibole by pyroxene and plagioclase is readily explained by decompression during the ascent of the magma towards the surface. Sulfide melt inclusions are generally absent from any phenocrysts in the extrusive andesites, suggesting that these magmas never exsolved a sulfide melt on a broad scale. Rapid degassing upon magma mixing suppressed the formation of a sulfide melt (Keith et al. 1997) and induced eruption selectively at times when volatile exsolution occurred locally in the magma chamber.

In intrusive rocks, melts of intermediate compositions are trapped preferentially by amphibole; plagioclase and quartz systematically contain inclusions of dacitic or more felsic composition, and pyroxene is absent from most intrusions. Thus, amphibole is likely to be the only phase to crystallize in significant amounts during mixing and andesite formation, outside the stability field of pyroxene. Pyroxene with melt inclusions of intermediate composition is only present in the Alto de la Blenda stock, the inferred volcanic conduit. In andesites, the

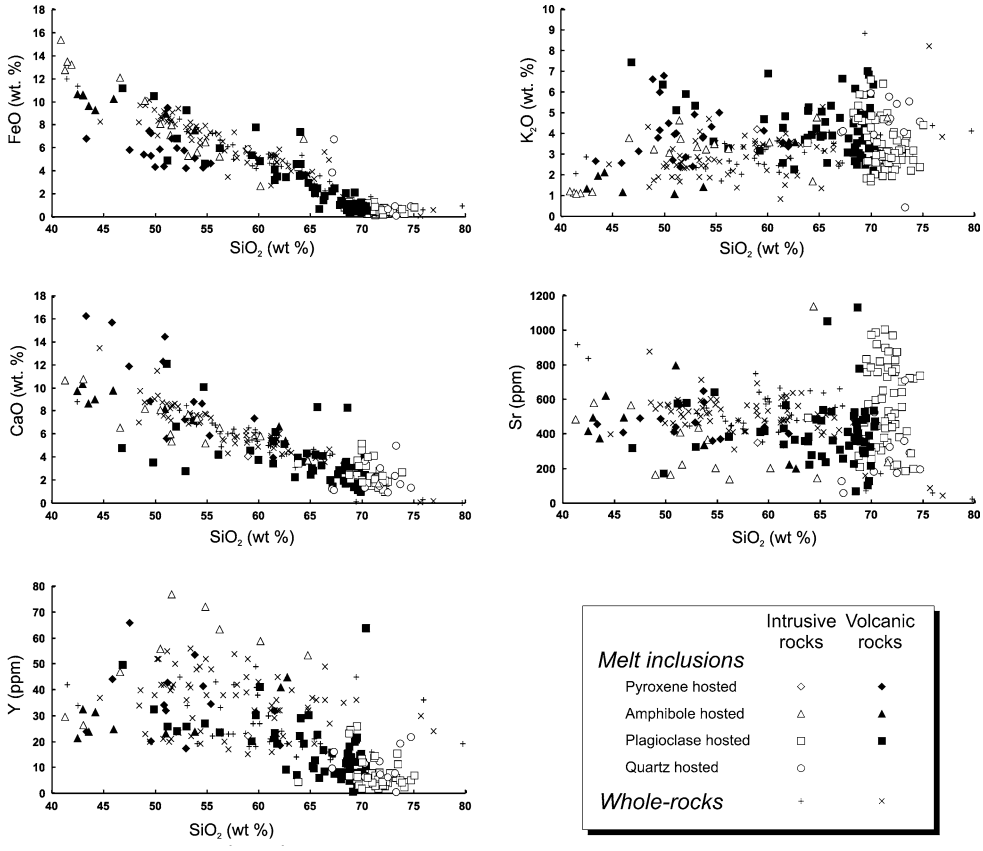

Fig. 4 Harker diagrams of selected major and trace element concentrations of silicate melt inclusions in the various host phases. Linear variations and bimodal distribution suggest that andesites are formed by mixing of a mafic and a felsic melt. Inclusions in intrusive and volcanic rocks follow similar trends, but depict systematic differences in their distribution

coexistence of amphibole and plagioclase and the absence of pyroxene indicate high water contents above 5.5 wt.% and pressures in excess of 250 MPa (Moore and Carmichael 1998). High water contents suggest that the source magmas for intrusions were not actively degassed during mixing. This is consistent with the positive correlation between the An-content of plagioclase and the silica content of the melt (Fig 6): high P_{H_2O}increases the anorthite content of plagioclase at constant melt composition (Johannes 1989; Housh and Luhr 1991). During crystallization of intrusions, this effect seems to dominate over the concurrent increase in the SiO_2 and Na_2O content of the evolving melt. Further evidence for phenocryst growth and mixing without significant degassing, and a prominent difference to the extrusive volcanic rocks, is the common association of sulfide melt inclusions with silicate melt inclusions of intermediate composition in amphibole phenocrysts

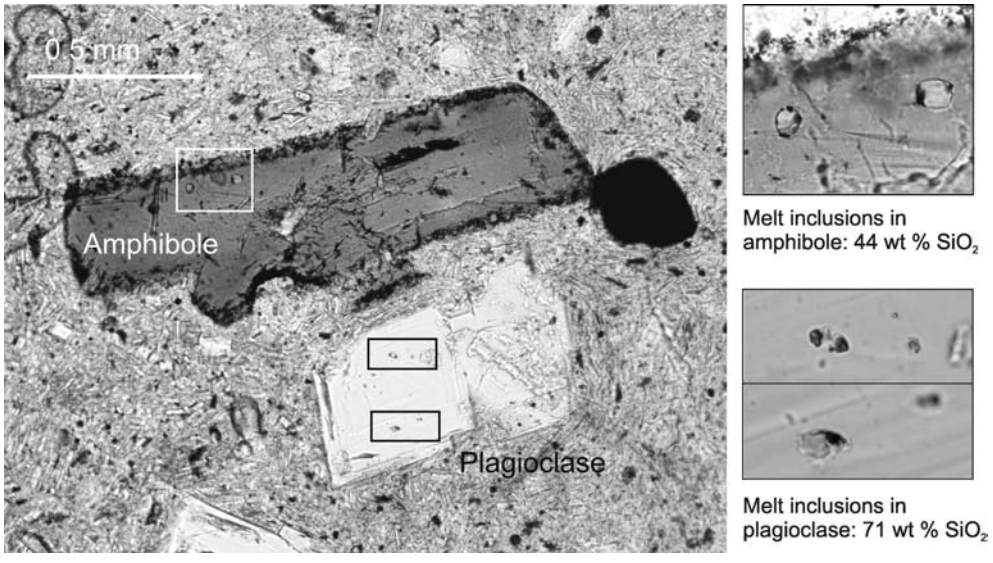

Fig. 5 Microphotograph of an andesitic rock containing amphibole and plagioclase phenocrysts. The amphiboles hosts melt inclusions with basaltic composition (44 wt.% SiO_2), the plagioclase rhyodacitic inclusions (71 wt.% SiO_2), indicating that the two minerals grew in highly contrasting melts, despite their common occurrence in andesitic magma

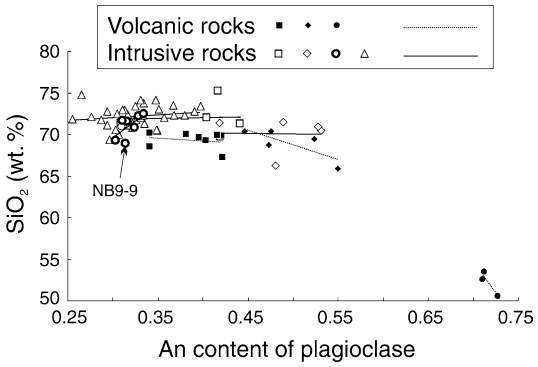

Fig. 6 SiO_2 content of melt inclusions in plagioclase as a function of the anorthite content of the host. Volcanic rocks show a negative correlation such that more mafic melts are trapped in more anorthite-rich plagioclase. This is true in individual crystals as well as over a range of host rock composition. In individual intrusive rocks (e.g., sample NB 9-9), the anorthite content of the plagioclase correlates positively with the SiO_2 content of the melt inclusion. This is likely to be due to the high water content of the melt which increases the anorthite content of the plagioclase in equilibrium with a given melt composition

of subvolcanic intrusions. Degassing would destabilize sulfides through the loss of sulfur to the volatile phase and suppress sulfide saturation.

The Alumbrera porphyry

Most of the stocks formed prior to Alumbrera show some hydrothermal alteration and Cu and Au enrichment to various extents, but only Alumbrera shows economic metal concentrations. It formed as a series of eight mappable intrusions (Fig. 2, Proffett 2003) showing a general evolution toward more mafic rocks, from early silica-rich dacites to late intermediate andesites (Ulrich and Heinrich 2001; Proffett 2003). This evolution of intrusion composition within the Alumbrera stock is taken as evidence for a chemically structured magma chamber, with initial extraction of silica-rich melts from the top and progressively more mafic melt from deeper parts of the chamber (Halter et al. 2004b). Emplacement of intrusions was probably caused by the buoyancy of silica- and volatile-rich magma in the roof zone of the magma chamber, together with structural focusing. Following a barren intrusion that pre-dates the porphyry stock, Cu–Au mineralization is associated with each magma pulse up to the fourth intrusion, with a general trend towards less intense alteration and mineralization with each pulse. Post-mineralization andesitic dykes that cut the stock are unaltered and barren, but they carry sulfide melt inclusions. The total amount of Cu deposited in the porphyry stock require a minimum source melt volume of approximately 15 km^3 of mafic magma (Halter et al. 2002a).

Based on U–Pb dating of zircon by laser-ablation ICPMS, Harris et al. (2004) suggested that the first mineralized (P2) intrusion at Alumbrera was emplaced at 8.0 ± 0.15 Ma. This age is significantly older than $^{40}Ar/^{39}Ar$ ages of 7.1 Ma determined by laser step-heating of biotite on the same intrusions (Sasso 1997) and was interpreted to indicate a gap of 1 million years between the first and subsequent mineralized intrusions in this stock. Given the extensive mixing and the long history of the magma chamber (Halter et al. 2004b) and the fact that zircon is a liquidus phase (Watson 1979), zircon phenocrysts could have formed some time before the actual emplacement of the magma (as shown previously in the Taupo Volcanic Zone by Charlier et al. 2003). A recent study by Oberli et al. (2004) reports high-precision zircon ages that are up to 5 Ma older than the time of solidification of a mid-crustal tonalitic magma chamber. Thus, the 8.0 Ma zircon age at Aumbrera is a maximum age for the first intrusion. Based on the petrographic similarity between the intrusions (Proffett 2003), we consider all mineralized intrusions to be emplaced within a restricted time frame, between 7.1 Ma and 6.8 Ma based on consistent Ar–Ar ages and zircons for the later intrusions. Emplacement of early intrusions at Alumbrera likely lowered the magma temperature, inducing additional growth of zircon crystals. Zircon crystals in subsequent intrusions have U–Pb ages indistinguishable from $^{40}Ar/^{39}Ar$ stepwise laser heating ages (Harris et al. 2004).

Laser-ablation inductively-coupled-plasma mass-spectrometry (LA-ICPMS) analysis of ore metals in melt inclusions and minerals

Analyses of silicate and sulfide melts were conducted using LA-ICPMS of entire inclusions without prior homogenization or exposure to the sample surface, following the signal deconvolution and quantification procedure of Halter et al. (2002b). Details of the analytical method are given by Gunther et al. (1998) and Heinrich et al. (2003) and tests of the accuracy of this analytical approach with regard to this study are discussed in Halter et al. (2004c) and Pettke et al. (2004). Results from silicate melt inclusions are fully documented in Halter et al. (2004b) and contributed to the reconstruction of the magma evolution reported above. Table 1 shows the sample location and a brief description.

Sulfide melt inclusions (Fig. 3) were analyzed for their Cu and Au contents. Such inclusions are almost exclusively present in amphiboles from unaltered intrusive rocks that also host silicate melt inclusions with andesitic compositions. Sulfide melt inclusions are notably absent from minerals other than amphibole and from volcanic rocks, with two exceptions: a volcanic rock (NB9) contains sulfide melt inclusions in highly corroded amphibole crystals and another volcanic rock (NB31B) contains sulfide melt inclusions in plagioclase and pyroxene. Primary sulfides could never be identified in the matrix of either volcanic or intrusive rocks.

Table 1 Samples used for melt inclusion analysis

Sample	Location	Coordinates	Rock	Main phenocrysts	Melt inclusion hosts	Age (Ma)
Volcanic rocks						
NB 5A (99)	Agua Tapada	3 432 150/ 6 986 132	Basaltic andesite	Plagioclase, amphibole, pyroxene, spinel	Pyroxene, plagioclase	~8.0
NB 9 (99)	Agua Tapada	3 432 152/ 6 986 061	Andesite	Plagioclase, amphibole, pyroxene, spinel	Pyroxene, plagioclase	8.05 ± 0.37
NB 15 (99)	Agua Tapada	3 431 830/ 6 986 611	Andesite	Plagioclase, amphibole, spinel	Plagioclase	7.78 ± 0.28
NB 31A (99)	Agua Tapada	3 432 185/ 6 986 330	Basaltic andesite	Plagioclase, amphibole, pyroxene, spinel	Amphibole, pyroxene	~8.0
NB 5B (00)	Tampa Tampa	3 439 726/ 6 982 690	Basaltic andesite	Plagioclase, amphibole, pyroxene, spinel	Amphibole, plagioclase	~9.5
NB 6 (00)	Tampa Tampa	3 439 620/ 6 983 031	Andesite	Plagioclase, amphibole, pyroxene, spinel	Pyroxene, plagioclase	9.4 ± 0.3
NB 31B (00)	Tampa Tampa	3 441 116/ 6 984 182	Andesite	Plagioclase, amphibole, spinel	Amphibole, plagioclase	9.0 ± 0.2
NB 49 (00)	Las Pampitas	3 437 623/ 6 978 949	Basaltic andesite	Plagioclase, amphibole, pyroxene, spinel	Plagioclase	~9.7
22-1KL	Agua Tapada	3 431 494/ 6 987 727	Dacite	Plagioclase, biotite, amphibole, quartz	Plagioclase	7.37 ± 0.35
Intrusive rocks						
ML 3/ML 5	Bajo el Durazno	3 441 803/ 6 982 705	Andesite	Plagioclase, amphibole, pyroxene, spinel	Amphibole, plagioclase	~8.2
ML 39	Las Pampitas	3 436 367/ 6 979 725	Dacite	Plagioclase, biotite, amphibole, quartz	Plagioclase, quartz	7.22 ± 0.28
9-9 (99)	Lomo Morado	3 430 154/ 6 986 387	Rhyodacite	Plagioclase, biotite, amphibole, quartz	Plagioclase	6.14 ± 0.05
ML 9	Alto de la Blenda	3 433 805/ 6 979 450	Andesite	Plagioclase, amphibole, pyroxene, spinel	Pyroxene	7.5 ± 0.20
ML 41	Macho Muerto	3 432 345/ 6 982 720	Rhyodacite	Plagioclase, biotite, amphibole, quartz	Plagioclase	6.26 ± 0.15
ML 44	Agua Tapada	3 433 388/ 6 986 310	Dacite	Plagioclase, biotite, amphibole, quartz	Plagioclase, quartz	7.39 ± 0.17
ML 47	Chilca	3 433 100/ 6 978 850	Andesite	Plagioclase, amphibole, pyroxene, spinel	Amphibole	7.94 ± 0.11
BLA 67	Alumbrera	Alumbrera P4	Andesite	Plagioclase, amphibole, spinel	Amphibole, plagioclase	6.78 ± 0.15
TU 10	Alumbrera	Alumbrera P3	Dacite	Plagioclase, biotite, amphibole, quartz	Quartz	6.83 ± 0.07
NB 32 (00)	Tampa Tampa	3 441 167/ 6 984 256	Andesite	Plagioclase, amphibole, spinel	Amphibole, plagioclase	9.0 ± 0.3

Ages are Ar–Ar ages described in Halter et al. (2004a)

Copper and gold contents of silicate and sulfide melt inclusions

The abundance of Cu in silicate melt inclusions displays a very large variation that can only be depicted on a logarithmic scale (Fig. 7), sharply contrasting with the simple mixing trend of all other elements that closely mimic the composition of bulk rocks (Halter et al. 2004b). In further contrast with other elements, Cu is almost systematically more abundant in silicate melt inclusions than in bulk rocks with the same silica content. In particular, Cu contents of the most primitive melts are approximately 100–200 ppm, corresponding to two to five times the bulk Cu concentration in mafic rocks. In silica-rich melts, Cu-concentrations of 20–50 ppm in inclusions represent a similar enrichment over bulk rocks.

In volcanic rocks, very high Cu concentrations (up to 3,500 ppm) occur in melt inclusions hosted by plagioclase and pyroxene (sample NB9) with silica contents between 50 wt.% and 55 wt.%. These high concentrations occur consistently in some inclusion populations and cannot be related to heterogeneous entrapment. Thus, they suggest extreme local Cu-enrichment in some melts.

In intrusive rocks, melt inclusions of intermediate composition (50–65 wt.% SiO_2) are mostly trapped in amphibole and then have very low Cu-contents, with concentrations of a few parts per million and often below the limit of detection of 2–3 ppm. Such inclusions are systematically associated with small (< 10 μm), irregularly shaped sulfide melt inclusions. Only inclusions of intermediate composition in sulfide-free pyroxene from the Alto de la Blenda stock have Cu-contents of several tens of parts per million, comparable to those of volcanic rocks and consistent with the interpretation that this stock was the main conduit during volcanic activity. Silica-rich melt inclusions in intrusive rocks

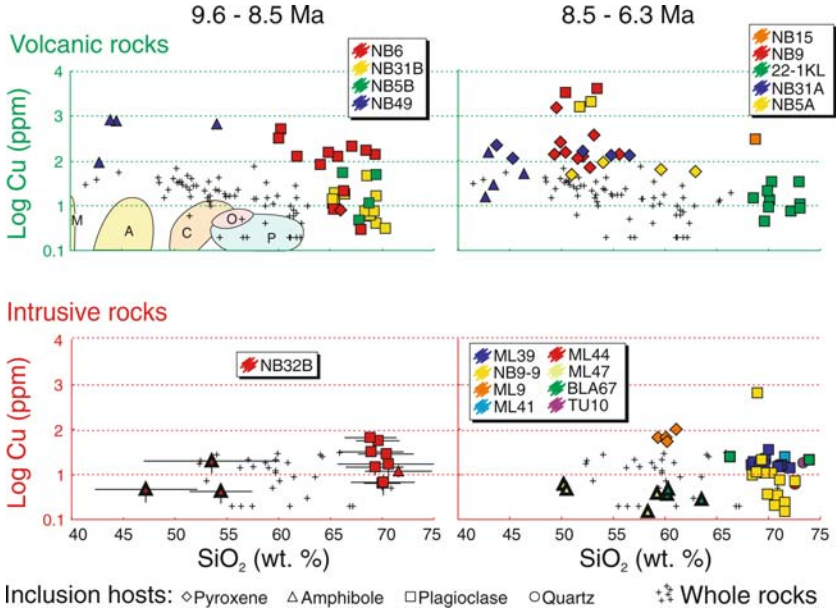

Fig. 7 Cu concentrations as a function of the SiO_2 content in silicate melt inclusions (from various host phases), bulk rocks and mineral phases (fields labeled M, A, O, C and P for magnetite, amphibole, orthopyroxene, clinopyroxene and plagioclase, respectively). *Bold symbols* are inclusions that co-exist with sulfide melt inclusions. Inclusions are generally richer in Cu than bulk rocks, suggesting Cu-loss during crystallization. Only silicate melt inclusions co-existing with sulfide melt inclusions are strongly depleted in Cu due to scavenging of Cu (and Au) by the sulfide liquid. This occurs only in andesitic melts, and Cu-depleted inclusions are only present in amphibole. The lower Cu content of silica-rich melt inclusions over mafic melt inclusions cannot be explained by fractionation as none of the solid phases contains any significant amount of Cu

have Cu concentrations between 20 ppm and 50 ppm but contain no sulfides.

Analyses of sulfide melt inclusions, present in amphiboles from three intrusive stocks (Bajo el Durazno, Chilca and Alumbrera) are shown in Table 2 and Fig. 8. These are mainly iron sulfides (pyrrhotite) with Cu contents up to several weight percentage. Gold could be measured in the largest inclusions, where limits of detection are as low as 0.1 ppm. In samples ML3/5 (Durazno) and ML47 (Chilca), the copper content is homogeneous, at 1.1 and 0.6 wt.% Cu respectively. Gold concentrations are approximately constant between 1 ppm and 2 ppm. In a post-ore dyke of the Alumbrera stock (BLA67), copper concentrations in sulfide melt inclusions are highly variable, ranging from below 3 ppm to 9.4 wt.%. These Cu concentrations are inversely correlated with the Au content (Fig. 8). In some inclusions from this sample, only the Au/Cu ratio was measured to improve the limit of detection. Element concentrations were obtained by assuming that they follow the same negative correlation between Au and Cu as determined in other inclusions of the same sample. Important to note is that the Cu/Au ratios in the sulfide melt inclusions are, on average for each sample, overlapping with those measured in the highest-temperature hydrothermal brines at Alumbrera (Ulrich et al. 2001) and in the bulk ore (Fig. 8).

All phenocrysts were analyzed for their Cu content to determine their potential in controlling the behavior of ore metals during melt evolution. Results are given in Table 3 and show that none of the silicate minerals nor magnetite incorporates significant amounts of Cu. Indeed, for a vast majority of the analyses, Cu is below the detection limit of a few parts per million. These results are shown by contours for the various minerals in Fig. 7 and imply that the Cu budget of the system is dominated by interactions between silicate melts, sulfide melts and hydrothermal fluids only.

Sources and sinks for Cu and Au

Volcanic rocks

Copper concentrations of bulk volcanic rocks in FNVC are lower that Cu concentrations measured in other ore-forming systems (Dilles 1987), but similar to other calc-alkaline rock suites (Ewart 1982) containing ~50 ppm in mafic rocks and decreasing to ~5 ppm in rhyodacites. This decrease in the Cu-content cannot be explained by the fractionation of oxide or silicate phenocrysts, because laser-ablation ICPMS analyses show that none of the phenocryst phases contains sufficient Cu to lower its concentration during magma evolution (Fig. 7) given that all rocks contain >50% groundmass by volume. Even phenocryst-poor bulk rocks show a consistent two to fivefold depletion in Cu compared to the melt, indicating that most of the Cu was lost from the magma during solidification. Given that copper and gold have a strong tendency to partition into an exsolving volatile phase, either an ore-forming brine (Ulrich et al. 1999) or a volcanic vapor phase (Candela and Holland 1984; Heinrich et al. 1992; Hedenquist et al. 1993; Lowenstern

Table 2 Measured element concentrations (with uncertainties) or element ratios in sulfide melt inclusions

Sample	FeS (wt.%)	Cu (wt.%)	Au (ppm)	Au/Cu (*10,000)
BLA67/7/SA3				12.20
BLA67/7/SA4				20.77
BLA67/7/SA7				18.10
BLA67/7/SA8				36.02
BLA67/7/SA11				2.55
BLA67/7/SA12				0.19
BLA67/8/SA1	93.00	4.51	< 1.30	
BLA67/8/SA2	95.66	2.80	0.21	
BLA67/8/SA3	98.23	1.14	< 0.48	
BLA67/8/SA4	95.91	2.64	< 0.55	
BLA67/8/SA7	85.43	9.39	< 1.62	
BLA67/8/SA8	99.73	0.17	0.41	
BLA67/8/SA9	98.89	0.72	0.44	
BLA67/8/SA10	98.53	0.95	< 0.37	
BLA67/8/SA11	99.42	0.38	1.23	
BLA67/8/SA12	97.73	1.46	< 0.53	
BLA6778/SA13	95.57	2.85	1.90	
BLA67/8/SA14	97.98	1.31	< 0.13	
BLA67/8/SA15	98.17	1.18	< 0.48	
BLA67/8/SA16	96.78	2.08	0.33	
BLA67/8/SA17	96.80	2.07	< 0.65	
BLA67/8/SA18	95.80	2.71	0.37	
BLA/8/SA20	98.21	1.15	< 0.22	
BLA67/9/SA1	96.80	2.06	< 5.91	
BLA67/9/SA2	99.46	0.35	0.86	
BLA67/9/SA4	98.26	1.12	< 0.34	
BLA67/9/SA6	94.27	3.69	0.24	
BLA67/9/SA7	90.18	6.33	< 0.47	
ML3/10/SA4	98.32	1.08	< 0.77	
ML3/9/SA6	98.46	1.00	4.33	
ML3/9/SA8	98.35	1.06	< 1.95	
ML3/9/SA9	97.49	1.62	0.69	
ML3/9/SA10	97.51	1.61	< 4.00	
ML3/9/SA11	98.24	1.13	1.12	
ML47/3/SA2	99.03	0.62	1.00	
ML47/3/SA3	98.82	0.76	< 0.80	
ML47/3/SA4	98.98	0.66	< 1.78	
ML47/3/SA5	98.05	1.26	< 2.85	
ML47/3/SA6	99.08	0.59	< 2.36	
ML47/4/SA7	99.39	0.39	0.29	
ML47/4/SA8	99.12	0.57	< 0.60	
ML47/4/SA10	99.17	0.54	< 1.22	
ML47/4/SA11	99.79	0.13	< 0.28	
ML47/4/SA13	99.25	0.48	< 0.34	
ML47/4/SA15	98.44	1.01	< 0.97	
ML47/4/SA14	99.26	0.48	1.71	
ML47/4/SA16	99.45	0.36	1.04	
ML47/5/SA17	99.24	0.49	< 0.48	
ML47/5/SA18	99.31	0.44	0.80	
ML47/5/SA19	99.41	0.38	3.33	
ML47/5/SA20	98.70	0.84	0.39	
ML47/5/SA21	99.93	0.05	< 0.37	
ML47/6/SA22	98.17	1.18	0.85	
ML47/6/SA23	99.46	0.35	0.90	
ML47/6/SA24	99.08	0.59	1.48	
ML47/6/SA25	99.16	0.54	< 0.59	
ML47/6/SA26	99.75	0.16	0.58	

Uncertainties (1σ): FeS ±2–5%, Cu ±0.2–2 %, Au ±40–80% < 0.59: below limit of detection

1993; Ulrich et al. 1999; Bodnar et al. 2002), the best explanation for this Cu-loss is a removal through an exsolving magmatic volatile phase during intrusion or eruption. Silicate melt inclusions thus provide a better measure of the amount of Cu initially available in the magmas, and this concentration was higher in the andesitic melt than in average andesitic rocks.

Magmatic sulfides are absent in the approximately 100 samples taken from volcanic units, with the exception of two samples only (NB31B and NB9), which contain sulfide melt inclusions in texturally relictic amphibole. The andesitic flow NB31B is the only biotite-bearing volcanic rock emplaced at an early stage (9.0 Ma). It is likely to have been extruded through a satellite conduit (i.e., the biotite-bearing Tampa Tampa stock, NB32), representing an evolution distinct from that of the main Alto de la Blenda system. The andesite NB9 contains strongly resorbed amphibole phenocrysts hosting sulfide melt inclusions (Fig. 3), as characteristic otherwise for intrusive rocks. In the same sample, silicate melt inclusions in plagioclase and pyroxene depict extreme Cu-concentrations up to 3,500 ppm (Fig. 7), but without sulfide melt inclusions. Thus, this andesite carries characteristics of intrusive and extrusive rocks and probably resulted from local mixing between both types of magmas. Resorption of sulfides during ascent through S-loss during degassing is responsible for the local enrichment of a small melt fraction to unusually high Cu concentrations.

Intrusive rocks

Sulfide melt inclusions are very rich in Cu (up to 9.6 wt.%) and Au (up to 4.3 ppm) while coexisting silicate melt inclusions of intermediate composition are highly depleted in Cu, with concentrations close to, and often below, the analytical limit of detection of a few parts per million (not shown in Fig. 7). This suggests that Cu (and Au) partitioned almost entirely into the sulfide melt wherever such a sulfide phase saturated in the magma (Halter et al. 2002a). This is consistent with experimental data that shows a strong preference of Cu for sulfides compared with silicate liquids (Jugo et al. 1999). Assuming a Cu content similar to those in melt inclusions from volcanic rocks prior to sulfide saturation, >95% of the ore metals are extracted from the surrounding silicate melt by the sulfides. Concentrations of a few weight percentage in the sulfide melt versus a few parts per million in the silicate melt yield partition coefficients for Cu between the sulfide and the silicate liquid of the order of 10,000. Given the high Au content of sulfide melt inclusions, it is presumably behaving the same way, although its concentration in silicate melt inclusions of a few tenth of micrometers could not be determined.

Silicate melt inclusions of dacitic and more silica-rich compositions are not associated with sulfide melt inclusions and their Cu content is of the order of a few tens of parts per million. Thus, dacitic magmas generating intrusions that host the Alumbrera deposit were not saturated with sulfides. The only intrusion at Alumbrera

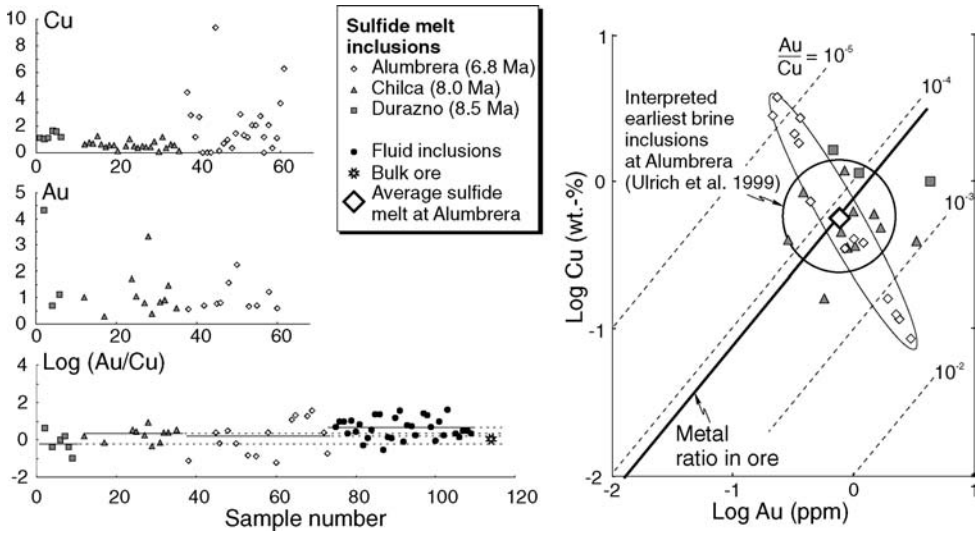

Fig. 8 Ore-metal concentrations and Cu/Au ratios in sulfide melt inclusions (Halter et al. 2002a) and fluid inclusions (Ulrich et al. 1999). Also shown are the metal ratios in early fluid inclusions in the Alumbrera deposit. Similar Cu/Au ratios in sulfide and fluid inclusions suggest a common magmatic source

carrying amphiboles with sulfide melt inclusions is the unaltered andesite dike emplaced last in this stock.

Texturally early high-temperature fluid inclusions associated with the ore-forming event in the Alumbrera deposit are high-temperature brines (~50% salinity, entrapped in pre-ore vein quartz at $T > 700°C$; Ulrich et al. 2001), containing Cu and Au in the same concentration ratio as the bulk ore. The same Cu/Au ratio is also recorded by the sulfide melt inclusions in barren porphyry intrusions of the FNVC (Halter et al. 2002a) and, in particular, in the late, unaltered andesitic intrusions of the Alumbrera stock (Fig. 8). The combined textural and metal-ratio data, therefore, indicate that the magmatic sulfides and the ore fluids share a common magmatic source.

Discussion: the formation of a copper-mineralizing magmatic-hydrothermal fluid

Combination of field evidence and results from the analytical study of silicate and sulfide melt inclusions constrain the behavior of Cu and S during magma evolution. We now use this information to discuss the sequence of processes that led to the formation of porphyry- mineralizing ore fluids.

Evolution of the ore-forming magma chamber

Phase equilibria require that the mafic component of the magma mixing process in the FNVC carried at least 6 wt.% of water at pressures of 350 MPa (Halter et al. 2004b), and the actual water contents might have been even higher. Thus, a large proportion of the water present in the system was introduced by this mafic, mantle-derived magma, and may ultimately be derived from the subducting slab. In the subvolcanic magma chamber, the mafic magma mixed with rhyodacitic melt, generating magmas of andesitic composition that locally exsolved droplets of sulfide melt. Magma mixing resulted in a hybrid assemblage of phenocrysts which were partly out of equilibrium with the mixed silicate melt.

The main volcanic activity ceased around 7.5 Ma, possibly as a result of a change in the tectonic regime from extensional (Sasso and Clark 1998) to compressional. Volcanic activity over 2.1 million years implies that the magma chamber was re-charged with hot magma, at least episodically, to prevent the bulk of the magma reservoir from complete crystallization. Some 0.4 million years after completion of the protracted extrusive volcanism, magmas were extracted from a progressively cooling magma chamber through sites of local structural weaknesses. At Alumbrera, the emplacement of increasingly more mafic magma within a short time period suggests a layered magma chamber at this stage, from which successively deeper magma batches were extracted (Fig. 9). We consider the first intrusion at Alumbrera to be part of this event and that the entire stock was formed in a short period of time, presumably between 7.1 Ma and 6.8 Ma, consistent the maximum U–Pb age of 8.0 Ma in zircon for the first, and 7.2 Ma for the second intrusion (Harris et al. 2004), the $^{40}Ar/^{39}Ar$ age of biotite providing a minimum age of the early intrusion (Sasso 1997) and interpretation from field evidence (Proffett 2003).

Sulfur budget and sulfide saturation

The evidence described above shows that mixing of mafic and rhyodacitic magma induces sulfide saturation in the resulting andesite, which is consistent with experimental data (e.g., O'Neill and Mavrogenes 2002) showing reduced sulfide solubility in melts of intermediate silica content. Saturating sulfide melts in the magma chamber have a composition close to FeS (with approximately 32 wt.% S) and contain an average of

Table 3 Copper concentration of phenocryst phases (in ppm)

	Intrusive rocks			Volcanic rocks		
	Sample	Cu	Uncertainty (%)	Sample	Cu	Uncertainty (%)
Plagioclase	ML5	< 14		NB31	< 1.6	
		56	21		< 2.3	
		< 109			< 2.4	
	NB32	< 0.8			< 2.8	
		< 1.7			< 3.7	
		< 0.3			< 2.1	
		< 1.1			< 1.7	
		< 3.2			< 0.2	
		< 3.1			< 1.8	
		< 4.1			2.3	45
		< 1.2			< 2.0	
		< 3.6			< 1.7	
		< 3.0			< 1.2	
	ML39	< 1.9		NB6	1.6	39
		< 44			< 1.9	
		< 1.2			< 1.5	
		< 2.7			2.6	56
		< 2.5			2.0	64
	ML41	< 8.0			1.7	34
		< 8.1			3.3	45
		< 6.3			< 2.6	
		< 14			< 1.9	
		< 6.8			< 1.7	
		< 7.6			< 0.8	
		< 6.8		NB15	< 5.0	
		< 24			< 4.1	
		< 12		NB5	< 2.2	
		< 15			< 1.0	
		< 135			< 4.0	
		< 6.7			< 3.5	
		< 13			1.4	99
		< 6.8			< 3.9	
		< 8.3			3.3	32
		< 7.0			< 4.2	
		< 7.7			3.8	53
		< 5.2			< 3.3	
		< 5.1		NB49	< 0.8	
		< 5.9			< 1.6	
		< 6.1			1.2	77
		< 6.1			< 0.6	
		< 6.5			< 1.2	
		< 5.9			< 4.3	
		< 12		ML32	< 58	
		< 6.6			16	25
		< 7.1			< 39	
		< 11		22-1kl	< 8.4	
		< 8.1			< 4.7	
		< 9.4			< 1.8	
		< 5.5			< 1.8	
		21	29		< 3.4	
		< 7.4			< 0.6	
		< 7.3		NB15	< 3.0	
		< 1.8			< 3.5	
	NB9-9	< 1.2			< 3.6	
		< 2.1		NB6	< 3.7	
		1.3	40	NB9	10	11%
		< 0.9			< 1.5	
		< 1.0				
		< 1.5				
		< 2.2				
		< 0.7				
	BLA67	< 1.4				
		< 2.5				

Table 3 (Contd.)

	Intrusive rocks			Volcanic rocks		
	Sample	Cu	Uncertainty (%)	Sample	Cu	Uncertainty (%)
Amphibole	BLA67	< 4.5		NB31	< 16	
		< 2.7			< 1.7	
		< 4.3		NB6	< 1.8	
	ML47	< 1.9		NB5	< 5.3	
		2.5	71		14	45
		< 2.0			< 11	
		< 2.7			6.8	25
	NB32	0.8	46	NB173	20	7
		0.9	59		14	5
		< 2.4				
		< 2.3				
		1.1	22			
	ML3	< 2.9				
		< 6.5				
		< 6.6				
Pyroxene	ML9	2.5	22	NB6	< 1.1	
				NB5	3.0	32
					3.2	32
					6.8	27
					11	10
					20	16
				NB173	3.9	25
				NB9	5.9	32
					3.2	10
				ML32	< 3.7	
Quartz	ML39	< 1.0				
		< 2.6				
		< 4.7				
		< 4.5				
	ML44	< 8.0				
		< 4.3				
	TU10	< 0.9				
		< 3.8				
		< 0.8				
		< 0.8				
		< 0.6				
		< 2.1				
		< 0.6				
Magnetite	BLA67	0.23	43%			
		< 0.38				
		< 0.22				
		3.10	23%			

Uncertainties are one standard deviation of the analytical uncertainty < 69.10: below limit of detection

0.8 wt.% Cu. The silicate inclusion data demonstrates that the formation of sulfide melt reduced the Cu content of the mixed (~andesitic) silicate melt from ~100 ppm to a few ppm. For this process to occur, the andesitic melt requires ~4,000 ppm S to account for the average S/Cu ratio of 40 in the sulfide melt. This is far above the sulfur solubility in a reduced, mafic melt, which is around 2,000 ppm, as estimated from experimental data by Carroll and Rutherford (1985) for the pressure, temperature and composition of the mafic melt in this volcanic complex (350 MPa, 1,000°C, 13 wt.% FeO; Halter et al. 2004b). Likewise for the rhyodacitic melt, sulfur solubility as sulfate at sufficiently oxidized conditions would be around 2,700 ppm only (Carroll and Rutherford 1985) at 350 MPa, 900°C and 4 wt.% FeO (Halter et al. 2004b). Equal amounts of the mafic and the rhyodacitic magmas would result in a mixture containing about 2,350 ppm total S, and 8 wt.% FeO at 950°C. At the estimated pressure of mixing (200 MPa; Halter et al. 2004b) and an oxygen fugacity close to the NNO buffer, the experimental sulfur solubility in the mixed melt is 600 ppm (Carroll and Rutherford 1985). Thus, mixing between a sulfide-saturated mafic and reduced melt and a sulfate-saturated silica-rich and oxidized melts can lead to exsolution of about 1,750 ppm S as sulfide. However, this is less than half the amount of S required to generate the high S/Cu ratio of ~40 in the sulfide melts.

Thus, an additional source of ~2,250 ppm of sulfur must be invoked, at least for those regions of the magma chamber from which the subvolcanic intrusions were extracted. This extra sulfur source can either be added

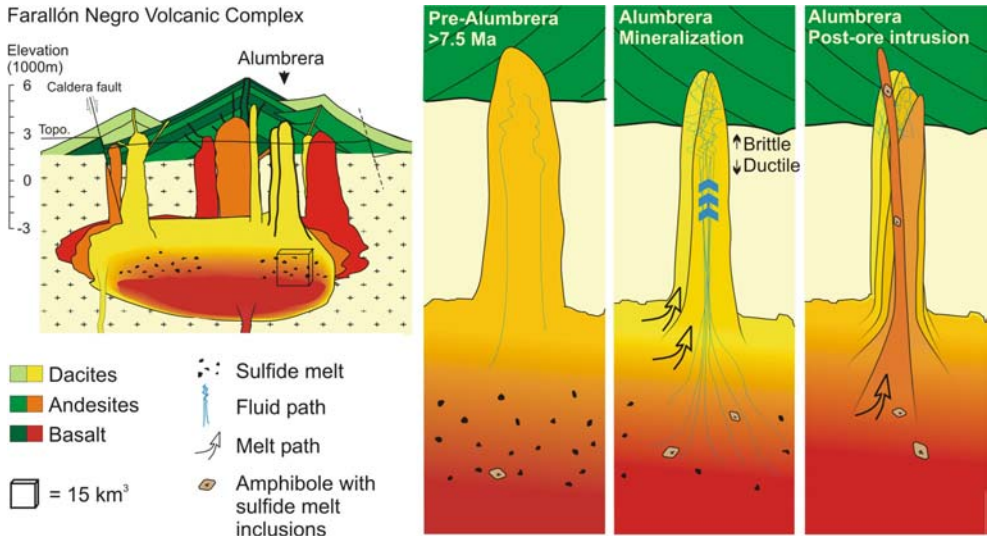

Fig. 9 Model for the formation of the Alumbrera deposit. The cross section represents a reconstruction of the FNVC (to scale) at the time of formation of the Alumbrera porphyry. Copper and gold poor fluids are first extracted from sulfide-understated magma at the top of the stratified magma chamber as long as the chamber was heated by the input of fresh magma (prior to 7.5 Ma). Intrusions that form the Alumbrera stock are extracted from successively deeper parts of the magma chamber and show evolution towards more mafic magmas. Fluid pulses generated after the chamber has cooled, for approximately 0.4 Ma, come from andesitic magmas that contain sulfides. Degassing destabilizes the sulfide liquid that releases its metal load to the fluid phase. This fluid mineralized dacitic magma extracted from shallower levels. The source magma for the mineralizing fluid is emplaced after the mineralizing event. The minimum volume of magma required to account for the amount of Cu in the deposit is represented by the *box* of 15 km^3

(1) by injection of a sulfide saturated mafic magma into the chamber, (2) by a separate S-rich volatile phase ascending from a larger reservoir of mafic magma, or (3) it may be present in the form of anhydrite as phenocrysts in the felsic melt.

Mafic melts could carry sulfide, as solid or as liquid, from the mantle to upper crustal levels, similar to the suggestion of Tomkins and Mavrogenes (2003) for silica-rich partial melts of the crust. This scenario is unlikely in the Farallón Negro complex because none of the volcanic rocks contain sulfide melt inclusions. Our evidence shows that sulfides saturate only upon mixing in some parts of the upper-crustal magma chamber.

Ascent of sulfur-rich gas from a layered magma chamber has been invoked previously to account for the large excess of SO_2 released during some volcanic eruptions e.g., Mount Pinatubo (Hattori 1993; Wallace and Gerlach 1994; Keppler 1999). Hattori (1996) suggested that the lower, mafic parts of the chamber could release S-rich fluids that rise buoyantly through the chamber and 'condense' into sulfide melt in the contact zone to an overlying more silica-rich magma. These sulfides will scavenge all local Cu and possibly a contribution of metals from the ascending volatile phase itself. Addition of S through a volatile phase can only solve the mass-balance problem if this fluid contains a ratio of sulfur to copper higher than S/Cu ~40 measured in the sulfide melt inclusions. Such a volatile phase could contain S in the form of H_2S and/or SO_2. If the latter dominates, an additional reductant will be required in the mixing zone where sulfide melt separation occurs.

An alternative source of excess sulfur could be solid sulfate crystals contributed by the felsic magma component to the mixing process. Previous studies of andesitic to rhyodacitic systems have reported anhydrite as a magmatic phase (Pallister et al. 1992; Hattori 1993; Kress 1997; Audétat et al. 2004; Parat et al. 2002), attesting high but not well-quantified bulk sulfate contents in such magmas. To account for the 'missing' ~2250 ppm S in the form of solid anhydrite crystals, the original felsic melt must have been exceptionally sulfate-rich, probably implying a specialized protolith for partial melting in the lower crust.

Unless the missing sulfur is added by an unusually reduced, deep volatile phase containing dominantly H_2S (Walshe et al. 2003), both mechanisms of sulfur addition to the zone of magmatic sulfide saturation require a reductant to generate S^{2-} from S^{4+} or S^{6+}. The only reductant of adequate concentration is Fe^{2+} in the mafic melt, which would be oxidized to Fe^{3+} leading to the crystallization of additional magnetite (Sun et al. 2004). Reduction of the required additional 2,250 ppm S^{6+} to S^{2-} would oxidize 2.9 wt.% Fe^{2+} and generate 8.3 wt.% magnetite in the hybrid andesitic magma. This is possible given the high concentration of FeO in the mafic melt, and consistent with the abundance of magnetite in the andesitic rocks.

Testing the two hypotheses requires a special sample preparation effort to identify relict anhydrite, which is expected to be preserved only as inclusions in plagioclase phenocrysts, i.e., the only crystallizing phase in the rhyodacitic magma. This has not been attempted so far. We favor anhydrite as a source for the excess sulfur as it would selectively enrich S in the melt and does not require the re-condensation of SO_2 gas into a sulfide

liquid. Either of the two processes emphasizes the important observation by Hunt (1991), who pointed out that porphyry systems are primarily major S anomalies, in which the enrichment factor of S is 10 to 100 times higher than the enrichment factor of Cu, compared to the average concentration of the two elements in the continental crust. Given the small amount of S that can exsolve during magma mixing, the addition of excess anhydrite might even be a prerequisite for the formation of a S-rich fluid capable of producing the large amount of sulfides and anhydrite present in porphyry–Cu systems. Areas of porphyry ore formation might then be areas of andesite magmatism involving partial melting of a crust capable of generating exceptionally sulfate-rich partial melts.

Copper budget

As the Cu content of the mafic magma is about ten times higher than that of the felsic component, most of the Cu is brought into the system by this mafic magma, probably from the mantle. The source for Au is less well constrained, and a contribution from the siliceous melt component (probably derived from melting of the lower crust) is possible and consistent with the common occurrence of Au-rich porphyry copper deposits above thick continental crust at some distance from the subduction zone.

Melt inclusions in volcanic rocks indicate that the average andesitic melt contained approximately 100 ppm Cu. This is four to five times more that the Cu content measured in the bulk rock and suggests that most of the Cu (~75 ppm) has been lost during magma degassing upon eruption. Based on the estimated volume of extruded magma of ~750 km^3(Halter et al. 2004a) and assuming that the magmas prior to eruption contained about 70% melt, this amounts to some 150 Mt of Cu that where lost to the atmosphere and hydrosphere during the entire lifetime of the volcanic complex, equating to ~50 times the economic Cu reserves of the Alumbrera deposit (Proffett 2003). Thus, Cu dispersion rather than concentration seems to be the prevailing process even in this ore-forming magmatic system, and special conditions within the magma chamber and at the depositional site are required to generate an economic ore deposit.

Volatile saturation and generation of the ore fluid

We suggest that the poor Cu and Au mineralization in early intrusions of the FNVC results from the fact that volatile exsolution was restricted to small regions within the upper parts of the chamber (Fig. 9). After the supply of fresh magma had ceased and extrusive activity had stopped (possibly aided by a change in stress regime surrounding the magma chamber), the bulk of the magma chamber cooled and progressively crystallized as a whole. After ~0.4 Ma of cooling, the pressure drop induced by the emplacement of the early most intrusions at Alumbrera generated massive exsolution of a relatively dense chloride-rich volatile phase from the bulk of the residual melt in a major part of the chamber, inducing hydro-fracturing and stockwork veining in the porphyry neck (Ulrich et al. 2001; Fig. 9). Subsequent intrusions were associated with their own alteration and mineralization event, as recorded by a repeatedly opened vein network (Ulrich and Heinrich 2001; Proffett 2003). Each mineralization event thus extracted a new pulse of fluid from the magma chamber. Precipitation of Cu-sulfides requires that the fluids cooled to $T < 420°C$ (Hezarkhani and Williams-Jones 1998; Ulrich et al. 2001) implying that successive intrusions cooled prior to emplacement of the next intrusion, which is easily possible in the time span of ~0.3 million years.

Magmatic sulfides are absent from the matrix of all rock types, indicating that sulfides were destabilized in the residual melt prior to solidification of the intrusive rocks. In conjunction with the low copper content in the bulk rocks, this observation shows that unprotected sulfides in the igneous matrix were resorbed during degassing of the residual melt, liberating Cu, Au, S and Fe to the volatile phase (Spooner 1993; Keith et al. 1997; Halter et al. 2002a). Destabilization of the sulfides is a likely result of volatile loss of the magma though the combined effect of sulfur loss and oxidation (H_2 loss). In the extrusive magmas, mixing and the exsolution of a low-density volatile phase probably happened almost simultaneously, so that sulfide exsolution rarely occurred. By contrast, in the intrusions, magmas mixed at higher pressures allowing a sulfide melt to form without immediate volatile saturation. The volatile phase, separating slightly later as a result of wholesale crystallization of the magma chamber, is likely to be a saline fluid of higher density, which can transport large concentrations of ore metals as well as sulfur in both oxidation states.

Microanalysis of fluid inclusions show that the input fluid at Alumbrera has similar metal ratios as the sulfide melt formed upon mixing (Ulrich et al. 1999). Most likely therefore, the sulfides represent the direct precursor metal host for the generation of highly metal-charged ore brines (Spooner 1993; Keith et al. 1997; Larocque et al. 2000; Halter et al. 2002a). These sulfides release their metal load to the volatile phase upon bulk dissolution of the sulfides during magma degassing. As a result, Cu and Au are quantitatively transferred into the ore-forming fluid phase (and thus not fractionated), explaining similar metal ratios in the sulfide melt and the fluid.

This process has important implications, not only for ore genesis but possibly also for practical exploration. It implies that the dacitic intrusions hosting the mineralization are not representing the source magma from which most of the ore fluid and its metal load were exsolved. Rather, the dacitic porphyry intrusions were derived from the uppermost part of the magma cham-

ber, while the fluids were released from a much larger mass of more mafic magma present deeper down within the layered magma chamber (Fig. 9). Late intrusions at Alumbrera are weakly mineralized not only because the fluid supply was exhausted, but also because all the sulfide liquid was consumed, except for the droplets included in the amphibole phenocrysts. The relatively mafic (~andesitic) porphyry dykes emplaced late in the Alumbrera stock, after hydrothermal Cu–Au-mineralization, are the most likely samples of the magma that acted as the main fluid and metal source. The magma carries relicts of the sulfide melts as inclusions in amphibole phenocrysts. These inclusions can be analyzed as the most representative material for the relative amount of Au and Cu available in the source region of the ore-forming fluids. Such post-mineralization, sulfide-bearing mafic magmas are not only present at Alumbrera, but were also described in the giant Bingham porphyry deposit, where Keith et al. (1997) interpreted them to be representing a potential metal source for the mineralization. At Bingham, the ore is also hosted by a much more felsic quartz-monzonite porphyry (Redmond et al. 2001).

Our interpretation of a mafic to hybrid andesitic magma source for the porphyry-mineralizing fluids is based on widespread features of all igneous rocks in the FNVC, together with the composition of the ore fluid characterized by numerous inclusion assemblages in the Bajo de la Alumbrera deposit (Ulrich et al. 2001). Harris et al. (2003) recently proposed an alternative interpretation, reporting compositions of nine fluid inclusions and seven melt inclusions trapped in high-temperature quartz veins from the deposit. Three of the fluid inclusions are reported to contain high Cu concentrations of 49,430, 73,570 and 95,680 ppm, while other inclusions in the same sample contain as little as 150 ppm. Based on these data, the authors suggest that such fluid—melt inclusion populations represent the exsolution event of the ore-forming brine and subsequent ore formation at temperatures between 750° and 550°C. This is inconsistent with several published and ongoing studies at Alumbrera and elsewhere. First, the melt inclusions contain between 12 wt.% and 14 wt.% K_2O, which is two to three times the concentration in the endmember felsic melt in the FNVC. Such melts can only result from extreme, and probably local, fractionation. Indeed, such melts could not be identified anywhere else, implying that they can only be a very subordinate mass of the entire volcano-plutonic complex. Mass-balance precludes that such specialized melts can generate the large mass of fluid necessary to form the Alumbrera deposit. Moreover, our extensive data set shows no evidence for Cu enrichment by fractionation (Fig. 7). Second, the interpretation by Harris et al. (2003) of Cu–Fe-sulfide precipitation at near-magmatic temperatures (750–550°C) is in conflict with Cu-solubility data (Hezarkhani et al. 1999) and with extensive fluid-compositional data from Alumbrera (Ulrich et al., 2001), and more recently from Bingham (Landtwing et al. 2004), which demonstrate that bornite and chalcopyrite saturation is only reached after cooling of the fluids to ~400°C.

Conclusions

The formation of the Bajo de la Alumbrera porphyry deposit is the last major event in the protracted igneous evolution of the FNVC, which was dominated by mixing of hydrous basalt and rhyodacitic melts. Ore formation occurred by the extraction of host dacitic magma from the upper part of a compositionally structured magma chamber, immediately followed by the extraction of ore fluid from the underlying mixed to mafic layer. Formation of the deposit required a large amount of magmatic fluid, a mechanism to enrich this fluid in ore metals, and the cooling of a focused fluid flux to approximately 400°C to allow Cu–Fe-sulfide precipitation.

The main source of Cu is a mafic melt rising from the mantle and carrying approximately 200 ppm Cu. The gold source is less clear but may involve the felsic magma component. Over most of the history of the FNVC, Cu was lost by extensive degassing associated with the volcanic activity. About 50 times the amount of Cu present in the Alumbrera deposit was lost to the atmosphere prior to ore formation. Thus, concentration of Cu into a spatially restricted volume required particular conditions within the magma chamber and the fluid plumbing system. In contrast to continually degassing extrusive magmas, the magmas emplaced as subvolcanic intrusions systematically saturated a sulfide melt during magma mixing. These sulfides scavenged >95% of the Cu and the Au from the ambient silicate liquid. The high S/Cu ratio (around 40) measured in these sulfides, requires about 4,000 ppm of S in the mixed andesitic magma, which is well above the concentration that can be contributed as dissolved S in either the mafic or the silica-rich magma components. An additional sulfur source is therefore required. The andesite was either enriched in SO_2 by a separate volatile phase, or, more likely, the silica-rich magma contained anhydrite phenocrysts. This excess sulfur may be a key to the formation of the Alumbrera and similar deposits. Given that Cu content of the magmas is not anomalously high, the formation of porphyry-type Cu deposits may require an anomalously S-rich, not a Cu-rich source.

All the stocks in the complex are altered, thus volatiles appear to have exsolved from the magma chamber each time a set of intrusions was emplaced in the subvolcanic environment. However, stocks generated during volcanic activity and while the system was continuously heated through input of new magma are only slightly mineralized. For these stocks, either the amount of fluid was too small or the fluid did not extract sufficient Cu and Au from the magmas. The key to the formation of the Alumbrera porphyry deposit is that the magma chamber was allowed to cool for 0.4 million years before ore formation. Thus, volatile saturation

could occur in the bulk of the magma chamber, including the andesitic magmas present in deeper parts of the reservoir and hosting sulfide melt. Degassing of this andesitic magma destabilized magmatic sulfides, rapidly releasing significant amounts Cu and Au to the exsolving fluid phase.

This model leads to a conclusion of fundamental significance and of practical importance to exploration. The dacitic intrusions, and other intermediate to felsic intrusions hosting other porphyry deposits, are not likely to represent the magma from which the ore fluid was exsolved. Thus, information extracted from phase assemblages and melt inclusions in the mineralized intrusions are not representative for the conditions at which the ore fluid was generated. The actual fluid source is an andesitic or even basaltic magma, which is present in the deeper parts of the magma chamber and may not always be emplaced at the erosion level of the deposit. At Alumbrera, andesitic magmas intruded after mineralization carry sulfide melt inclusions in amphibole, and these intrusions are the best candidates for yielding information on the conditions of ore-fluid formation. Cu/Au ratios measured in the sulfide melt inclusions of these rocks provide the best indication of the Cu/Au ratio in the mineralizing fluid and the ore body. Systematic LA-ICPMS analysis of sulfide melt inclusions in such post-ore intrusions can therefore be applied to predict potentially Au-rich porphyry systems during the early stages of exploration in similar magmatic-hydrothermal systems elsewhere.

Acknowledgements This study was partly supported by ETH research funds and by the Swiss National Science Foundation (grant 20-59544-99 to CAH). Extensive logistic support was granted by Minera Alumbrera Ltd. and MIM Exploration, and we would like to thank Dave Keough and Steve Brown, in particular, for their help. Mario Alderete and Nicolás Montenegro, from YMAD (Tucumán, Argentina) provided authorization to access the Farallón Negro exploration prospect and on site support. Many thanks also to Jim Webster and Bernd Lehmann, whose comments helped to improve the manuscript significantly.

References

Allmendinger RW (1986) Tectonic development, southeastern border of the Puna plateau, Northwestern Argentine Andes. Geol Soc Am Bull 97:1070–1082

Audetat A, Gunther D, Heinrich CA (1998) Formation of a magmatic-hydrothermal ore deposit: insights with LA-ICP-MS analysis of fluid inclusions. Science 279:2091–2094

Audetat A, Pettke T, Dolejs D (2004) Magmatic anhydrite and calcite in the ore-forming quartz- monzodiorite magma at Santa Rita, New Mexico (USA): genetic constraints on porphyry-Cu mineralization. Lithos 72:147–161

Bain N (2001) Petrological and geochemical contribution to the Farallón Negro Volcanic Complex, NW-Argentina. Diploma Thesis. Swiss Federal Institute of Technology, Zurich, 92 pp

Bassi HGL, Rochefort G (1980) Estudio geologico del yacimiento cuproaurifero de la Alumbrera. Servicio Minero Nacional, Buenos Aires

Becker K (2001) Sm-Nd and Rb-Sr isotope geochemistry on the magmatic source of the igneous rocks in the Farallón Negro Volcanic Complex, NW Argentina. Diploma Thesis. Swiss Federal Institute of Technology, Zurich, 103 pp

Bodnar RJ, Rapien RH, Simmons S, Szabo CS, Wood CP, Sutton SR (2002) Neo-natal porphyry copper system at White Island, New Zealand. Geochim Cosmochim Acta 66:A86–A86

Candela PA, Holland HD (1984) The partitioning of copper and molybdenum between silicate melts and aqueous fluids. Geochim Cosmochim Acta 48:373–380

Carroll MR, Rutherford MJ (1985) Sulfide and sulfate saturation in hydrous silicate melts. J Geophys Res 90:C601–C612

Charlier BLA, Peate DW, Wilson CJN, Lowenstern JB, Storey M, Brown SJA (2003) Crystallisation ages in coeval silicic magma bodies: U-238-Th- 230 disequilibrium evidence from the Rotoiti and Earthquake Flat eruption deposits, Taupo Volcanic Zone, New Zealand. Earth Planet Sci Lett 206:441–457

Coughlin TJ, O'Sullivan PB, Kohn BP, Holcombe RJ (1998) Apatite fission-track thermochronology of the Sierras Pampeanas, central western Argentina; implications for the mechanism of plateau uplift in the Andes. Geology (Boulder) 26:999–1002

Dilles JH (1987) Petrology of the Yerington Batholith, Nevada—evidence for evolution of porphyry copper ore fluids. Econ Geol 82:1750–1789

Dungan MA, Wulff A, Thompson R (2001) Eruptive stratigraphy of the Tatara-San Pedro complex, 36°S, southern volcanic zone, Chilean Andes: reconstruction method and implications for magma evolution at long-lived arc volcanic centers. J Petrol 42:555–626

Ewart A (1982) The mineralogy and petrology of tertiary-recent orogenic volcanic rocks; with special reference to the andesitic-basaltic compositional range. In: Thorpe RS (ed) Andesites; orogenic andesites and related rocks. Wiley, Chichester, pp 25–95

Guilbert JM (1995) Geology, alteration, mineralization, and genesis of the Bajo de la Alumbrera porphyry copper-gold deposit, Catamarca Province, Argentina. In: Pierce FW, Bolm JG (eds) Porphyry copper deposits of the American Cordillera: Arizona Geological Society Digest, vol 20. Arizona Geological Society, Tucson, pp 646–656

Gunther D, Audetat A, Frischknecht R, Heinrich CA (1998) Quantitative analysis of major, minor and trace elements in fluid inclusions using laser ablation inductively coupled plasma mass spectrometry. J Anal Atom Spectrom 13:263–270

Gustafson LB, Hunt JP (1975) The porphyry copper deposit at El Salvador, Chile. Econ Geol Bull Soc Econ Geol 70:857–912

Halter WE, Pettke T, Heinrich CA (2002a) The origin of Cu/Au ratios in porphyry-type ore deposits. Science 296:1844–1846

Halter WE, Pettke T, Heinrich CA, Rothen-Rutishauser B (2002b) Major to trace element analysis of melt inclusions by laser-ablation ICP-MS: methods of quantification. Chem Geol 183:63–86

Halter WE, Bain N, Becker K, Heinrich CA, Landtwing M, VonQuadt A, Bissig T, Clark AH, Sasso AM, Tosdal RM (2004a) From andesitic volcanism to the formation of a porphyry-Cu-Au mineralizing magma chamber: The Farallón Negro Volcanic Complex, northwestern Argentina. J Volcanol Geotherm Res (in press)

Halter WE, Heinrich CA, Pettke T (2004b) Laser-ablation ICP-MS analysis of silicate and sulfide melt inclusions in an andesitic complex II: magmas genesis and implications for ore-formation. Contrib Mineral Petrol 147:397–412

Halter WE, Pettke T, Heinrich CA (2004c) Laser-ablation ICP-MS analysis of silicate and sulfide melt inclusions in an andesitic complex I: analytical approach and data evaluation. Contrib Mineral Petrol 147:385–396

Harris AC, Kamenetsky VS, White NC, van Achterbergh E, Ryan CG (2003) Melt inclusions in veins: linking magmas and porphyry Cu deposits. Science 302:2109–2111

Harris AC, Allen CM, Bryan SE, Campbell IH, Holcombe RJ, Palin JM (2004) ELA-ICP-MS U-Pb zircon geochronology of regional volcanism hosting the Bajo de la Alumbrera Cu-Au deposit: implications for porphyry-related mineralization. Miner Deposita 39:46–67

Hattori K (1993) High-sulfur magma, a product of fluid discharge from underlying mafic magma—evidence from Mount-Pinatubo, Philippines. Geology 21:1083–1086

Hattori K (1996) Occurrence and origin of sulfide and sulfate in the 1991 Mount Pinatubo eruption products. In: Newhall Christopher G, Punongbayan Raymundo S (eds) Fire and mud; eruptions and lahars of Mount Pinatubo, Philippines, Philippine Institute of Volcanology and Seismology. University of Washington Press, United States, Quezon City, Philippines, pp 807–824

Hedenquist JW, Simmons SF, Giggenbach WF, Eldridge CS (1993) White-Island, New-Zealand, volcanic-hydrothermal system represents the geochemical environment of high-sulfidation Cu and Au ore deposition. Geology 21:731–734

Heinrich CA, Ryan CG, Mernagh TP, Eadington PJ (1992) Segregation of ore metals between magmatic brine and vapor—a fluid inclusion study using pixe microanalysis. Econ Geol Bull Soc Econ Geol 87:1566–1583

Heinrich CA, Pettke T, Halter WE, Aigner-Torres M, Audetat A, Gunther D, Hattendorf B, Bleiner D, Guillong M, Horn I (2003) Quantitative multi-element analysis of minerals, fluid and melt inclusions by laser-ablation inductively-coupled-plasma mass-spectrometry. Geochim Cosmochim Acta 67:3473–3497

Heinrich CA, Driesner T, Stefansson A, Seward TM (2004) Magmatic vapor contraction and the transport of gold from the porphyry environment to epithermal ore deposits. Geology 32:761–764

Hezarkhani A, Williams-Jones AE (1998) Controls of alteration and mineralization in the Sungun porphyry copper deposit, Iran: evidence from fluid inclusions and stable isotopes. Econ Geol Bull Soc Econ Geol 93:651–670

Hezarkhani A, Williams-Jones AE, Gammons CH (1999) Factors controlling copper solubility and chalcopyrite deposition in the Sungun porphyry copper deposit, Iran. Miner Deposita 34:770–783

Housh TB, Luhr JF (1991) Plagioclase-melt equilibria in hydrous systems. Am Miner 76:477–492

Hunt JP (1991) Porphyry copper deposits: Historical perspectives of genetic concepts and case histories of famous discoveries: economic Geology Monographs, vol 8. Economic Geology Publishing Co., Lancaster, pp 192–206

Johannes W (1989) Melting of plagioclase-quartz assemblages at 2-Kbar Water-pressure. Contrib Mineral Petrol 103:270–276

Jordan TE, Allmendinger RW (1986) The sierra pampeanas of Argentina: a moderne analogue of Rocky Mountain foreland deformation. Am J Sci 260:737–764

Jugo PJ, Candela PA, Piccoli PM (1999) Magmatic sulfides and Au:Cu ratios in porphyry deposits: an experimental study of copper and gold partitioning at 850°C, 100 MPa in a haplogranitic melt pyrrhotite intermediate solid solution gold metal assemblage, at gas saturation. Lithos 46:573–589

Keith JD, Whitney JA, Hattori K, Ballantyne GH, Christiansen EH, Barr DL, Cannan TM, Hook CJ (1997) The role of magmatic sulfides and mafic alkaline magmas in the Bingham and Tintic mining districts, Utah. J Petrol 38:1679–1690

Keppler H (1999) Experimental evidence for the source of excess sulfur in explosive volcanic eruptions. Science 284:1652–1654

Kesler SE, Chryssoulis SL, Simon G (2002) Gold in porphyry copper deposits: its abundance and fate. Ore Geol Rev 21:103–124

Kress V (1997) Magma mixing as a source for Pinatubo sulphur. Nature 389:591–593

Landtwing M (2004) Fluid evolution and ore metal precipitation at the Bingham porphyry Cu-Au-Mo deposit, Utah, deduced from cathodoluminescence imaging and LA-ICPMS microanalysis of fluid inclusions. PhD Thesis, ETH Zurich, Zurich, 126 pp

Larocque ACL, Stimac JA, Keith JD, Huminicki MAE (2000) Evidence for open-system behavior in immiscible Fe-S-O liquids in silicate magmas: Implications for contributions of metals and sulfur to ore-forming fluids. Can Mineral 38:1233–1249

Llambías EJ (1970) Geologia de los yacimientos mineros Agua de Dionisio, Prov. de Catamarca, Rep. Argentina. Revista de la Asociacion Argentina de Mineralogia Petrologia y Sedimentologia 1:2–32

Llambías EJ (1972) Estructura del grupo volcanico Farallon Negro, Catamarca, Republica Argentina. Revista de la Asociacion Geologica Argentina 27:161–169

Lowell JD, Guilbert JM (1970) Lateral and vertical alteration-mineralization zoning in porphyry ore deposits. Econ Geol Bull Soc Econ Geol 65:373–408

Lowenstern JB (1993) Evidence for a copper-bearing fluid in magma erupted at the Valley of Ten-Thousand-Smokes, Alaska. Contrib Mineral Petrol 114:409–421

Moore G, Carmichael ISE (1998) The hydrous phase equilibria (to 3 kbar) of an andesite and basaltic andesite from western Mexico: constraints on water content and conditions of phenocryst growth. Contrib Mineral Petrol 130:304–319

Oberli F, Meier M, Berger A, Rosenberg CL, Giere R (2004) U-Th-Pb and Th-230/U-238 disequilibrium isotope systematics: precise accessory mineral chronology and melt evolution tracing in the Alpine Bergell intrusion. Geochim Cosmochim Acta 68:2543–2560

O'Neill HSC, Mavrogenes JA (2002) The sulfide capacity and the sulfur content at sulfide saturation of silicate melts at 1400°C and 1 bar. J Petrol 43:1049–1087

Pallister JS, Hoblitt RP, Reyes AG (1992) A basalt trigger for the 1991 eruptions of Pinatubo Volcano. Nature 356:426–428

Parat F, Dungan MA, Streck MJ (2002) Anhydrite, pyrrhotite, and sulfur-rich apatite: tracing the sulfur evolution of an Oligocene andesite (Eagle Mountain, CO, USA). Lithos 64:63–75

Pettke T, Halter WE, Webster JD, Aigner-Torres M, Heinrich CA (2004) Accurate quantification of melt inclusion chemistry by LA-ICPMS: a comparison with EMP and SIMS and advantages and possible limitations of these methods. Lithos 78:333–361

Proffett JM (2003) Geology of the Bajo de la Alumbrera porphyry copper-gold deposit, Argentina. Econ Geol Bull Soc Econ Geol 98: 1535–1574 ; 1534 sheets

Redmond PB, Landtwing MR, Einaudi MT (2001) Cycles of porphyry dike emplacement, veining, alteration and mineralisation in the Bingham porphyry Cu-Au-Mo deposit, Utah. In: Piestrzynski A et al (eds) Mineral deposits at the beginning of the 21st century. Society for Geology Applied to Mineral Deposits (SGA). International, Krakow

Sasso AM (1997) Geological evolution and metallogenetic relationships of the Farallon Negro volcanic complex, NW Argentina. PhD Thesis. Queen's University, 843 pp

Sasso AM, Clark AH (1998) The farallón negro group, northwest Argentina: magmatic, hydrothermal and tectonic evolution and implications for Cu-Au metallogeny in the Andean back-arc. Soc Econ Geol Newslett 34:8–17

Sillitoe RH (1973) The tops and bottoms of porphyry copper deposits. Econ Geol Bull Soc Econ Geol 68:799–815

Sparks RSJ, Marshall LA (1986) Thermal and mechanical constraints on mixing between mafic and silicic magmas. J Volcanol Geotherm Res 29:99–124

Spooner ETC (1993) Magmatic sulfide volatile interaction as a mechanism for producing chalcophile element enriched, Archean Au-quartz, epithermal Au-Ag and Au skarn hydrothermal ore F fluids. Ore Geol Rev 7:359–379

Stefanini B, Williams-Jones AE (1996) Hydrothermal evolution in the Calabona porphyry copper system (Sardinia, Italy): the path to an uneconomic deposit. Econ Geol Bull Soc Econ Geol 91:774–791

Stults A (1985) Geology of the Bajo de la Alumbrera porphyry copper and gold prospect, Catamarca province, Argentina. Masters Thesis, University of Arizona, Tuscon, 75 pp

Sun WD, Arculus RJ, Kamenetsky VS, Binns RA (2004) Release of gold-bearing fluids in convergent margin magmas prompted by magnetite crystallization. Nature 431:975–978

Tomkins AG, Mavrogenes JA (2003) Generation of metal-rich felsic magmas during crustal anatexis. Geology 31:765–768

Ulrich T (1999) Genesis of the Bajo de la Alumbrera porphyry Cu-Au deposit, Argentina: geological, fluid geochemical, and isotopic implications. Doctoral Thesis, Swiss Federal Institute of Technology, Zurich, 207 pp

Ulrich T, Heinrich CA (2001) Geology and alteration geochemistry of the porphyry Cu-Au deposit at Bajo de la Alumbrera, Argentina, vol 96, p 1719, 2001, correctly printed in 2002. Econ Geol Bull Soc Econ Geol 97:1863–1888

Ulrich T, Gunther D, Heinrich CA (1999) Gold concentrations of magmatic brines and the metal budget of porphyry copper deposits. Nature 399:676–679

Ulrich T, Gunther D, Heinrich CA (2001) Evolution of a porphyry Cu-Au deposit, based on LA-ICP-MS analysis of fluid inclusions: Bajo de la Alumbrera, Argentina, vol 96, p 1743, 2001, correctly printed in 2002. Econ Geol Bull Soc Econ Geol 97:1888–1920

Urreiztieta M, Rosello EA, Gapais D, LeGorve C, Cobbold PR 1993. Neogene dextural transpression at the southern edge of the Altiplano-Puna (NW Argentina). In: IInd international symposium on andean tectonics, Oxford, pp 267–269

Wallace PJ, Gerlach TM (1994) Magmatic vapor source for sulfur-dioxide released during volcanic-eruptions—evidence from Mount-Pinatubo. Science 265:497–499

Walshe JL, Cooke DR, Cannell J, Frikken P, Hollings P, Masterman G, Skarmeta J, Camus F, Gow PA, Midgley G (2003) Physicochemical gradients and architectural constraints on fluid-mixing models of porphyry Cu formation. In: Eliopoulos DG et al (eds) Mineral exploration and sustainable development. Mill press, Athens, pp 419–422

Watson EB (1979) Zircon saturation in felsic liquids—experimental results and applications to trace-element geochemistry. Contrib Mineral Petrol 70:407–419

Wolf KJ, Eichelberger JC (1997) Syneruptive mixing, degassing, and crystallization at Redoubt Volcano, eruption of December, 1989 to May 1990. J Volcanol Geotherm Res 75:19–37